Available online at www.sciencedirect.com
ScienceDirect
Cement and Concrete Research 37 (2007) 680–690
Cement and Concrete Research

A method for measuring transient thermal diffusivity in hydrating Portland cement mortars using an oscillating boundary temperature

William M. Chirdon, Wilkins Aquino *, Kenneth C. Hover

School of Civil and Environmental Engineering, 220 Hollister Hall, Cornell University, Ithaca, NY 14853-3501, United States

Received 6 July 2006; accepted 26 January 2007

Abstract

The transient thermal diffusivity in early-age, type I Portland cement mortars is difficult to quantify because the exothermic reactions cause significant heat generation which complicates the analysis of heat transfer. This paper outlines the theory and setup for a method of determining the transient thermal diffusivity of Portland cement mortars by forcing an oscillating temperature on one side of the material and measuring the attenuation of the temperature oscillation with distance. This experimental method also controls temperature to acquire data over a specific and narrow temperature range. The method is illustrated using computer models and laboratory experiments on wet and dry sand and Portland cement mortar. The values of thermal diffusivity of sand and mortar determined by this method correspond well to values found in literature. This general method could be applied to other materials, including cement paste, concrete, reactive solids, or biological tissue with appropriate modification to the apparatus.

Keywords: Thermal diffusivity; Fresh concrete; Physical properties; Mortar; Temperature

1. Introduction

Modeling the generation and transfer of heat in early-age concrete is essential to understanding the material as a whole. The thermal history of concrete during hydration affects the rate and extent of the reaction and the ultimate properties of the specimen. Thermal gradients can cause internal stresses which can lead to cracking on a microscopic or catastrophic scale [1,2]. Hence, the temperature of concrete while it is hardening is a major design consideration, especially since the time–temperature history affects both strength and durability. Conversely, some information about the properties of concrete can be gleaned from temperature profiles and computer modeling [3].

Development of accurate heat transfer models requires accurate material properties. For modeling temperature profiles, thermal diffusivity is of paramount importance. The diffusivities of the component materials and of hardened concrete are easily acquired from standard experiments or literature values [4–11]. However, defining the thermal diffusivity of early-age concrete is complicated because it requires quantifying heat transfer while the hydration reactions generate heat as the specimen changes gradually from a liquid to a solid [2]. The few studies available on the heat transfer properties of fresh concrete, mortar, and cement yield contradictory results, and the diffusivity values acquired depend not only on the material, but also on the measurement technique [12]. No consensus has been reached as to whether thermal diffusivity and thermal conductivity increase, decrease, increase to a maximum value then decrease, or remain constant during the hydration process [12].

The authors hypothesize that many of the differences in the reported values for thermal diffusivity and conductivity are due to the complications arising from internal heat generation which complicate the heat transfer calculations. Published techniques often have minimal compensation, if any, for the errors caused by heat generation. This could lead to a systematic error where heat generation presents itself as an irregularity in apparent thermal diffusivity or conductivity.

* Corresponding author. Tel.: +1 607 255 3294.
E-mail address: wa27@cornell.edu (W. Aquino).

0008-8846/$ - see front matter © 2007 Elsevier Ltd. All rights reserved.
doi:10.1016/j.cemconres.2007.01.010

A further complication is that thermal properties for concrete and related materials are often published without mentioning the range of temperatures to which the specimen is subjected, even though the thermal properties of materials may have significant temperature dependencies. Ideally, one would like to have isothermal conductivity data at different temperatures to minimize the effects of heating and thermal gradients on the chemical and physical properties. Then, the thermal properties as functions of temperature and time could be reconstructed from multiple measurements at various set temperatures. However, heat generation makes perfectly isothermal analyses impossible, in addition to the fact that measurement of heat transfer properties requires thermal gradients.

Time dependence is another potential complication for measuring the thermal properties of Portland cement mortar or any other reactive system. The thermal properties are likely to change during the course of the experiment as the specimen undergoes chemical and physical changes. Before analyzing such a system, a successful experimental method must demonstrate that changes in thermal diffusivity over the duration of the experiment will not invalidate the assumptions upon which the analysis was based.

To address these issues, a new technique for measuring the diffusivity of Portland cement mortar has been developed. This method oscillates the temperature of one side of the specimen around a set temperature, so that the average temperature and amplitude of the oscillation are controlled and can be changed as experimental parameters. The propagation of the thermal oscillation through the specimen is used to calculate its thermal diffusivity. By using a small temperature oscillation instead of a heat pulse, the thermal diffusivity can be calculated over a narrow temperature range.

The conceptual and mathematical bases for this method are discussed in the next section. Computer simulations were used to demonstrate that this is a robust method for determining time and temperature-dependent thermal diffusivity in the presence of internal heat generation. Computer simulation was also used to optimize the design of the experiment and the algorithm of the data analysis. A series of laboratory experiments was then performed using concrete sand to quantitatively verify the method before performing experiments on early-age Portland cement mortars.

2. Theoretical background

2.1. Concept

The basis of the proposed method for measuring thermal diffusivity is related to the concepts of thermal lag and amplitude reduction arising from thermal mass effects in concrete [13]. If the temperature on one side of a specimen is forced to be a sinusoidal function, the thermal diffusivity can be readily calculated from the amplitude reduction and timing of the peaks of the thermal wave as it propagates through the specimen. A mathematical model, finite-element model, and an experimental schematic for this method are shown in Fig. 1.

2.2. Mathematical model

Thermal diffusivity can be calculated by measuring the amplitude reduction and time-lag of a sinusoidal thermal signal as follows. Consider the heat transfer problem illustrated in Fig. 1a. The specimen is in contact with a vertical wall on the left side that has a controlled, sinusoidal temperature profile over time. The proposed method uses temperature measurements over time at two arbitrary positions, x_1 and x_2, within the specimen to calculate thermal diffusivity.

The problem shown in Fig. 1a is defined in one spatial dimension and time. The mathematical initial-boundary value problem can be described by the governing energy conservation equation

$$\frac{\partial T}{\partial t} = \alpha(t)\frac{\partial^2 T}{\partial x^2} + g(t), \quad x\in(0,\infty),\ t\in[0,t_{\max}], \tag{1}$$

subject to boundary conditions at the left wall

$$T(0,t) = T_{\text{avg}} + T_{\text{amp}}\cos(\omega t), \tag{2}$$

and on the right side

$$\alpha(t)\frac{\partial T}{\partial x}\bigg|_{x\to\infty} = 0 \tag{3}$$

The initial condition for the above problem is expressed as

$$T(x,0) = T_{\text{ini}}. \tag{4}$$

In Eqs. (1)–(4),

- $\alpha(t)$ is the thermal diffusivity as a function of time (t) after water addition to the cement,
- $T(x,t)$ is the temperature as a function of distance from the wall (x) and time,
- $g(t)$ is the intrinsic heat generation rate per unit volume
- T_{avg} is the average temperature of the boundary, and
- T_{amp} is the amplitude of the sinusoidal boundary temperature oscillation,
- ω is the frequency of the oscillation (in radians per second), and
- T_{ini} is the initial temperature of the specimen.

The thermal diffusivity of a material can also be expressed in terms of the heat capacity per unit volume, C, and its thermal conductivity, k, as

$$\alpha = \frac{k}{C}. \tag{5}$$

In the definition of the above problem, the material is assumed to be isotropic and homogeneous. This assumption is valid if the spacing of the temperature measurements ($x_2 - x_1$) is much larger than any material discontinuities, particularly the size of coarse aggregate and any compaction voids. In addition, the thermal diffusivity was assumed to depend only on time and its potential dependence on the temperature was ignored in this derivation. Temperature dependence could potentially invalidate the derivation of Eqs. (10) and (13). However, neglecting the

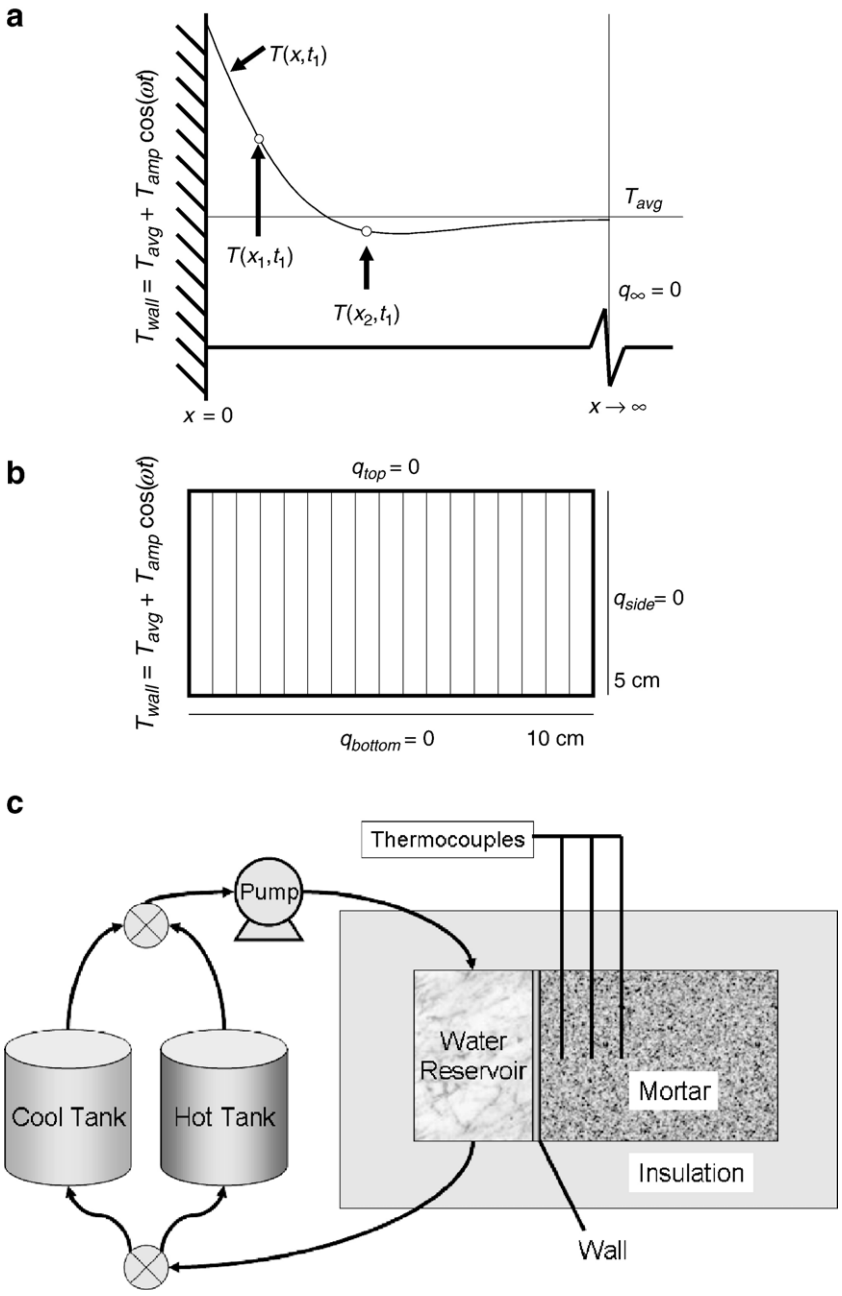

Fig. 1. a. Sketch of the mathematical model of the proposed method. The temperature at the left wall is defined as a sinusoidal function. Thermal diffusivity of a material can be calculated by the propagation of this wave at two arbitrary positions, x_1 and x_2. b. Finite-element model for the proposed experiment. The temperature on the left wall is controlled. The other boundaries are insulated and set to zero heat flux. c. A simplified schematic of the experimental method. Water from two baths set at two different temperatures is alternatively circulated in a reservoir next to the specimen.

temperature dependence in the derivation is permissible if the temperature dependence and temperature fluctuations are both small. This will be verified for the temperature fluctuation used in the experiment for reasonable values for material temperature dependence through computer simulation in Section 2.5.

The temperature dependence of the material can then be determined by running the specimens at different average temperatures.

After some time, one can assume that the transient, start-up features in the oscillation have passed (the length of this time is also studied in the computer simulation). At this point in the derivation, the internal heat generation $g(t)$ is assumed to be zero, and the thermal diffusivity is assumed to be constant, so that the harmonic analytical solution to the initial-boundary value problem in Eqs. (1) (2) (3) (4) can be derived as [14]

$$T(x,t) = T_{\text{avg}} + T_{\text{amp}} e^{-x\sqrt{\omega/2\alpha}} \cos(\omega t - x\sqrt{\omega/2\alpha}). \quad (6)$$

The temperature profile defined by Eq. (6) is plotted in Fig. 2 at two time points (200 s and 400 s). Although the time dependence of the diffusivity has been removed in the above equation, this time dependence can be reconstructed in a

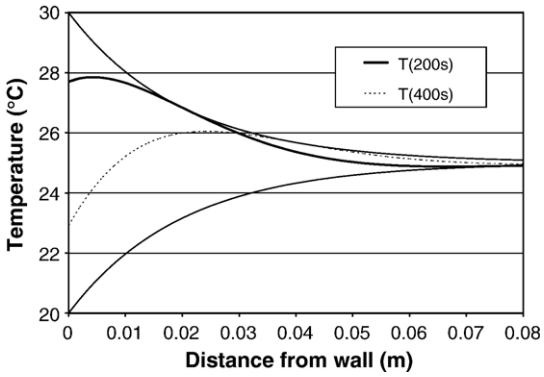

Fig. 2. Plot of Eq. (6) showing the temperature profile in a sample at two different times. Maximum and minimum values (thin solid lines) for the function over time are also plotted.

piecewise manner for given time intervals. The separation and removal of the effects of heat generation will also be discussed in Section 2.4.

The diffusivity can be calculated from Eq. (6) by using the temperature amplitude decay between two arbitrary, different points (x_1 and x_2) selected in the domain. To derive the relationship between thermal diffusivity and amplitude decay, the following procedure is followed. First, the amplitude of the temperature oscillation is measured at the two different positions. One should note that the local maxima and minima will occur at two different times, t_{peak1} and t_{peak2}, when

$$\cos(\omega t - x\sqrt{\omega/2\alpha}) = \pm 1$$

for x_1 and x_2. The amplitudes at x_1 and x_2 are then calculated as

$$A_1 = T\left(x_1, t_{\text{peak1}}\right) - T_{\text{avg}} = T_{\text{amp}} e^{-x_1\sqrt{\omega/2\alpha}} \tag{7}$$

and

$$A_2 = T\left(x_2, t_{\text{peak2}}\right) - T_{\text{avg}} = T_{\text{amp}} e^{-x_2\sqrt{\omega/2\alpha},} \tag{8}$$

respectively. Taking the ratio between these two amplitude yields

$$\frac{A_1}{A_2} = \exp\left[(x_2 - x_1)\sqrt{\frac{\omega}{2\alpha}}\right]. \tag{9}$$

Solving for the thermal diffusivity in Eq. (9) results in

$$\alpha = \frac{\omega}{2}\left(\frac{\Delta x}{\ln\left(\frac{A_1}{A_2}\right)}\right)^2. \tag{10}$$

where the quantity $\Delta x = x_2 - x_1$ has been introduced.

Alternatively, the thermal diffusivity can be calculated using the time-lag between the maximum peak temperatures at two arbitrary points, x_1 and x_2, as follows. First, take

$$\cos\left(\omega t_{\text{peak1}} - x_1\sqrt{\frac{\omega}{2\alpha}}\right) = \cos\left(\omega t_{\text{peak2}} - x_2\sqrt{\frac{\omega}{2\alpha}}\right). \tag{11}$$

Then,

$$\omega t_{\text{peak1}} - x_1\sqrt{\frac{\omega}{2\alpha}} = \omega t_{\text{peak2}} - x_2\sqrt{\frac{\omega}{2\alpha}} + 2n\pi, \quad n = 0,1,2,\ldots. \tag{12}$$

Setting $n=0$ and solving for the thermal diffusivity, α, yields

$$\alpha = \frac{\Delta x^2}{2\omega\Delta t^2}. \tag{13}$$

By setting $n=0$, the distance between x_1 and x_2 is implicitly assumed to be less than one thermal wavelength, and the time-lag between t_{peak1} and t_{peak2} is assumed to be less than one oscillation period. If the distance between x_1 and x_2 is greater than one thermal wavelength, then Δt must be corrected for by adding the integer value of the number of full wavelength distances between x_1 and x_2 multiplied by the period of the oscillation. Experimentally, however, x_1 and x_2 will typically be close together to retain an acceptable signal-to-noise ratio for the data at x_2, so this experimental consideration will keep x_1 and x_2 within one wavelength for most experimental designs. Therefore, the assumption that $n=0$ should be valid for most practical experiments. This assumption can be tested by inputting the frequency, Δx, and the lowest plausible thermal diffusivity value for the material into Eq. (13) and calculating the expected time-lag (Δt). If the resultant time-lag is less than one oscillation period, then one can safely assume $n=0$, and Eq. (13) can be used with the apparent time-lag. The $n=0$ assumption implied by calculations made via Eq. (13) can also be validated by checking with thermal diffusivity calculations based on Eq. (10).

2.3. Piecewise reconstruction of the thermal diffusivity and treatment of heat generation

In obtaining Eq. (6), the thermal diffusivity was assumed to be constant. However, the main interest in this work is to determine thermal diffusivity as a function of time. If the changes in thermal diffusivity are slower than the period of oscillation of the solution in Eq. (6), then Eqs. (10) and (13) can be used by assuming that the thermal diffusivity remains constant in time intervals Δt.

Heat generation was assumed to be zero to obtain the analytical solution shown in Eq. (6). This solution will be advantageously used to separate temperature changes due to heat generation in early-age Portland cement mortar. For narrow temperature ranges, the thermal diffusivity is assumed to be independent of temperature [15]. From this assumption, the initial-boundary value problem shown in Eqs. (1) (2) (3) (4) is linear and the principle of superposition applies. Let $T_{g(t)}(x,t)$ be the temperature field produced by heat generation with a constant boundary temperature of T_{avg}, and let $T_{\text{osc}}(x,t)$ be the temperature field resulting from the oscillating boundary temperature in a material without internal heat generation.

Then, using superposition, the observed temperature field in the body can be expressed as

$$T(x,t) = T_{g(t)}(x,t) + T_{\mathrm{osc}}(x,t). \quad (14)$$

The temperature field due to the boundary temperature oscillates around the temperature field resulting from the internal heat generation. The component $T_{\mathrm{osc}}(x,t)$ can then be obtained as

$$T_{\mathrm{osc}}(x,t) = T(x,t) - T_{g(t)}(x,t). \quad (15)$$

Once this temperature field has been extracted from the observed temperature field, it can be used with Eq. (10) or Eq. (13) to compute thermal diffusivity at different time intervals.

By taking the difference in $T_{\mathrm{osc}}(x,t)$ between a local maximum to a local minimum at a position, x_1, and dividing by 2, A_1 is defined over this narrow time interval. A_2 is similarly defined at position, x_2, over a slightly shifted, but overlapping time interval. The thermal diffusivity can then be calculated using the amplitude ratio $\left(\frac{A_1}{A_2}\right)$ and Eq. (10) over this time interval. The times at which the local maxima or minima occur can similarly be recorded to calculate the thermal diffusivity over this interval using the time-lag $(t_1 - t_2)$ and Eq. (13).

2.4. Extraction of peak amplitude and time

The primary challenge of the data collection and analysis is to extract the peak amplitudes and times so that thermal diffusivity can be calculated using Eq. (10) or Eq. (13). Raw data from the laboratory experiment (shown in Fig. 1c and detailed in Section 3) using Portland cement mortar is displayed in Fig. 3a. The three oscillating waveforms are the thermal histories at distances of 1 cm, 2 cm, and 3 cm from the temperature-controlled wall. The average temperature increases and the amplitude of the oscillation decreases as the observation point moves away from the wall. Thermal diffusivity can be calculated from temperature data collected at any two selected positions within the specimen.

The first step in the data analysis is to remove the fine noise, which can be accomplished by using various filtering strategies. In this work, a moving average of five data points (average temperature over a 50-second window) was used to smooth the function. Performing this moving-average function three times was sufficient to remove the fine noise in the data (this is necessary to prevent the false identification of peaks by the algorithm to be discussed later). Taking repeated moving averages of the waveform does slightly change the amplitude of the oscillation. However, since the change is proportional to the amplitude, the moving average will affect the amplitudes of any given wave form (A_1, A_2, A_3), but it will not affect the amplitude ratios of two waveforms (A_1/A_2), assuming the same number and type of moving-average functions are used on each waveform. From inspection of Eq. (10), one may note that calculation of thermal diffusivity requires accurate values for the amplitude ratio (A_1/A_2), while accurate determination of the individual amplitudes is not strictly necessary.

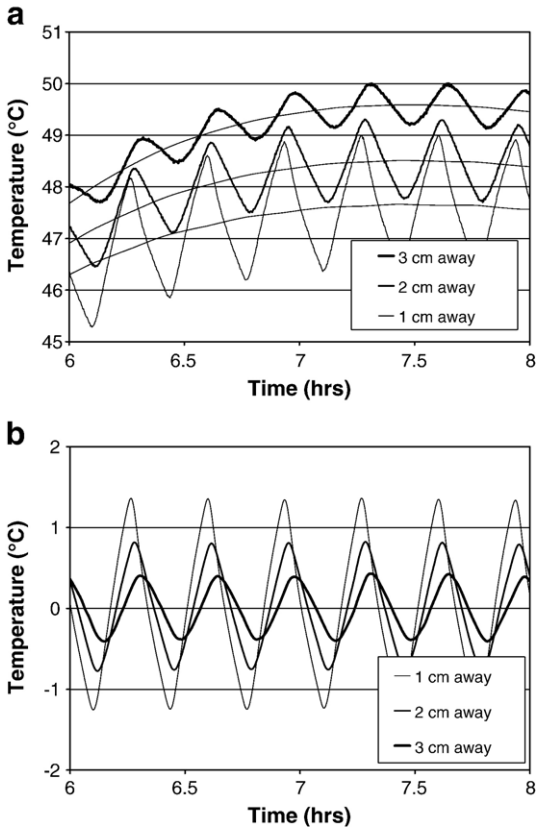

Fig. 3. a. Temperature data for three distances from the wall using the proposed method on Portland cement mortar. Moving averages of one period (20 min) are drawn through the raw data to define a baseline to be subtracted. b. Temperature data after applying a short-range (50 s) moving average to smooth the raw data and subtracting the long-range (20 min) moving average as a baseline.

The waveforms can be understood as a thermal signal, $T_{\mathrm{osc}}(x,t)$, superimposed over a baseline, $T_g(x,t)$, as expressed in Eq. (14). To remove the oscillating component of the waveform, a moving average of one period is performed. The computer models and the laboratory experiments were conducted using a period of 20 min. Fig. 3a shows the moving average of one period drawn through the data for each of the three waveforms. This one-period moving average is considered to be $T_g(x,t)$ which is the baseline to be subtracted. After performing 50-second moving averages to remove fine noise and subtracting the one-period, moving-average baseline, all that remains is $T_{\mathrm{osc}}(x,t)$, which is the thermal signal for calculating thermal diffusivity. $T_{\mathrm{osc}}(x,t)$ for the data in Fig. 3a is shown in Fig. 3b. The fine noise and baseline have been effectively eliminated, and the amplitude reduction and time-lag are now more pronounced.

After $T_{\mathrm{osc}}(x,t)$ has been isolated, the temperature differences divided by the sampling time (10 s) between each point can be used to define the slope between those points (this can be accomplished using a spreadsheet). Simple logical operations can then be used to identify times when the slope changes sign, corresponding to either a maximum or minimum value. The height/depth and time of this peak can then be recorded. Using this method, noise in the data can result in falsely identified

peaks. For this reason, effective noise elimination can greatly expedite the data analysis, since manual removal of false peaks from the data set is time-consuming. Once all of the peak heights/depths and times are recorded, the amplitude can be defined as half of the temperature difference between a maximum value and the next minimum value of temperature, or vice versa. This yields 2 amplitude readouts per oscillation period.

Once the amplitude as a function of time has been extracted for waveforms at two distances, the amplitude ratio for each oscillation can be used to calculate thermal diffusivity using Eq. (10). The difference in the time at which the peaks occurred between the two distances can also be used to calculate thermal diffusivity using Eq. (13).

2.5. Computer model

To explore the feasibility of the method described above before any physical experiments were performed, numerical simulations were carried out using the commercial finite-element software ABAQUS. This allowed for illustration of the concept, formulation of the data analysis, testing of assumptions, assessment of boundary effects, and optimization of design parameters before the experimental apparatus was constructed. While the thermal properties of fresh and hardened Portland cement mortars reported from different studies and applications vary significantly, the range of their values is approximately known. By using plausible values in the computer simulation, the experimental setup can be optimized. These simulations are particularly useful for testing and selecting experimental parameters such as ω, T_{amp}, x_1, and x_2.

A 2-D finite-element model of the proposed experimental setup was developed to be of similar size and shape to that of the equipment used in the experiment. The 2-D model consisted of a rectangular cell 5-cm tall and 10-cm wide as seen in Fig. 1b. The left wall had a specified average temperature of 26.86 °C (300 K) that oscillates with an amplitude of 5 °C as

$$T_{wall}(t) = 26.86 + 5\cos(6\pi\, t), ^{\circ}\mathrm{C} \quad (16)$$

while a zero heat flux (insulated) boundary condition was specified for the other sides.

The uniformly-distributed heat generation was modeled as a first-order reaction with parameters fitted to temperature data from previous experimental work [3] as

$$g(t) = 10319e^{-0.00005374t}\ \mathrm{W/m^3}. \quad (17)$$

The transient diffusivity used in the model,

$$\alpha = \frac{1 + (t/36{,}000)^4}{3{,}525{,}000}\ \mathrm{m^2 s}, \quad (18)$$

was designed to be approximately within the range of literature values [12] with the modification having a large, non-linear dependence on time.

The volumetric heat capacity was defined as a constant 3.525×10^6 J/m^3 K to be in the range of literature values [3,12]. The temperatures at 1 cm and 2 cm from the wall, shown in Fig. 4a, were used to calculate the thermal diffusivity as a function of time. The time and amplitude of each peak were extracted from $T_{osc}(x,t)$ for the thermal waveforms at the two specified locations and then were use to calculate thermal diffusivity via both Eqs. (10) and (13). The computed values are compared to the actual value used in the model in Fig. 4b. Before 1 h, the temperature profile is in transition from the initial state (Eq. (4)) to the state after the transient (start-up) effects have passed (Eq. (6)). Therefore, Eqs. (10) and (13) do not apply until this transition is complete. After 1 h, the start-up and transient aspects of the thermal profile have passed, and the thermal diffusivity can be calculated with 97% accuracy as seen in Fig. 4b. Therefore, in a laboratory experiment with comparable physical dimensions, experimental parameters, and material properties, the transient (non-steady) state effects on thermal diffusivity calculations should similarly become negligible after approximately 1 h.

The computer simulations were also used to assess the effect of input signals that depart from perfect sinusoids. Although sinusoidal temperature inputs are easy to construct mathematically, they can be difficult to achieve experimentally. From inspection of Fig. 1c, one can see if the volumetric flow rate of the circulating water becomes large

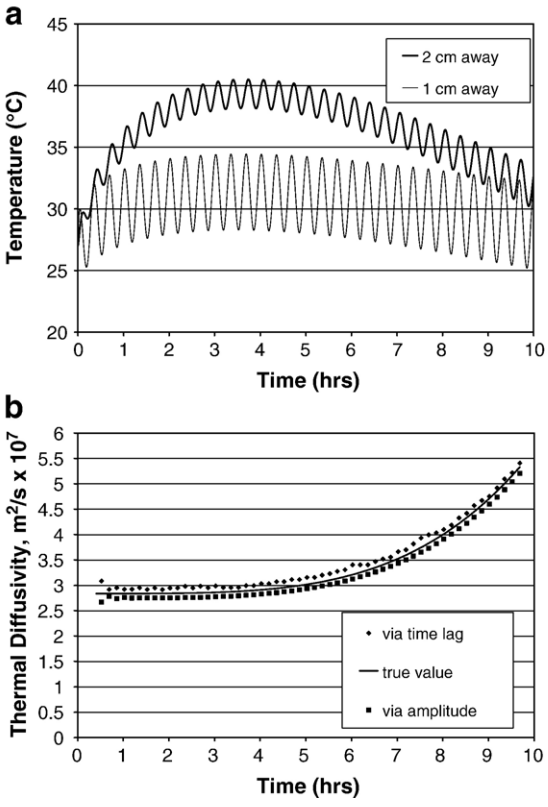

Fig. 4. a. Temperature at two distances from the wall in a computer simulation of a mortar being analyzed by the proposed method. b. Thermal diffusivity calculated using Eqs. (10) and (13) compared to the thermal diffusivity value input into the computer simulation.

relative to the volume of the water reservoir (resulting in a small residence time), the temperature of the water reservoir will simply alternate between the temperature of the two water baths, since the simple on/off valves are not variable. The alternating temperature of the wall, $T(0,t)$, may then resemble a rectangular pulse (shown as the 0-cm profile in Fig. 5a) and would not be a sinusoidal function as assumed in the mathematic model derived from Eq. (2).

The temperature and time dependence of the heat transfer properties was also addressed in this simulation. The thermal conductivity inserted into this model was temperature-dependent, changing by −0.01 W/m K/°C, and time-dependent, changing by −0.01 W/m K/h. This trial value for the temperature dependence of thermal conductivity was selected to be far greater than typical temperature dependencies for most materials [15] and is considered to be a worst case for potential temperature dependence. Heat capacity, C, is assumed to remain constant over time and temperature as in the previous computer simulation. Although this last assumption is not strictly true, it is acceptable for this simulation, which imparts time and temperature dependence on thermal conductivity (and transitively on thermal diffusivity) to assess the reliability of this method for materials with thermal properties that have dependencies on time and temperature.

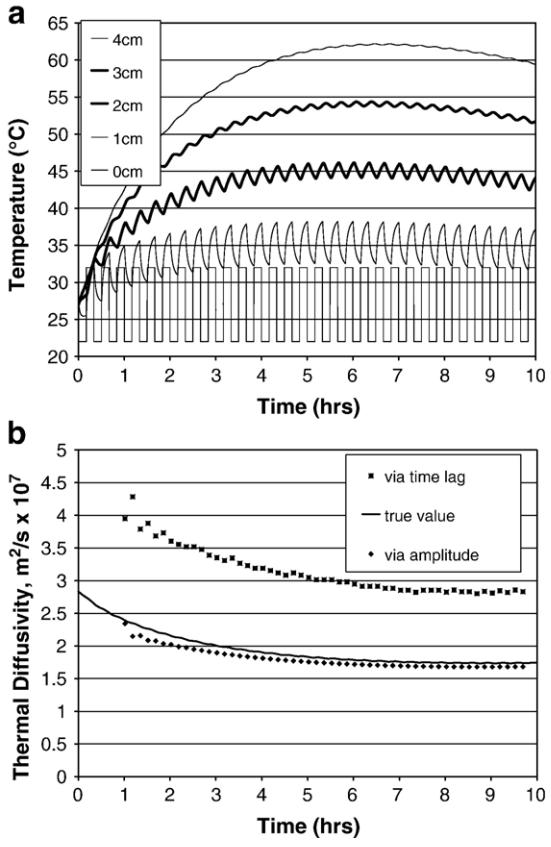

Fig. 5. a. Temperature profile for a material with a temperature-dependent thermal diffusivity. Also, the sinusoidal input function was replaced with a rectangular pulse function. b. Thermal diffusivity calculated by applying Eqs. (10) and (13) to the 2-cm and 3-cm distance data from Fig. 5a.

Fig. 5a shows the thermal waveform developing into what resembles a "saw-tooth" function and then becomes more sinusoidal. Note that thermal diffusivity values calculated from Eqs. (10) and (13) assume that the thermal waveforms at x_1 and x_2 are sinusoidal, and this becomes a better assumption when x_1 and x_2 are chosen further from the wall. The temperature profiles at 2 and 3 cm from the wall have become approximately sinusoidal as seen in Fig. 5a. Fig. 5b shows that thermal diffusivity could still be calculated with an accuracy of 95% relative to the input value after 4 h using the amplitude ratios (Eq. (10)) of temperature oscillations at the 2-cm and 3-cm positions. Despite the non-sinusoidal input, the waveforms at these positions were close enough to sinusoids to yield accurate results. This shows that thermal diffusivity calculations from Eq. (10) depend on the waveforms at x_1 and x_2 being sinusoidal, but the temperature profile at the wall can significantly deviate from a sinusoid.

However, the timing of the maximum peak changes as the waveform changes shape, which introduces error in the diffusivity calculations based on time-lag between peaks (Eq. (13)). This causes thermal diffusivity values calculated using time-lag to have a significant error of 68% after 4 h. For this reason, the calculations using experimental data in Section 4 are performed on the basis of amplitude ratios, since the result is far less dependent on the sinusoidal input assumption and time resolution.

Note also that the analytical solution was derived on the basis of a semi-infinite domain (see Fig. 1a), while the numerical simulations were carried in a bounded domain (see Fig. 1b). The computer simulations revealed that, for the system and geometry studied, the presence of finite boundaries had a negligible influence in the calculation of the thermal diffusivities using the proposed approach.

3. Laboratory experiments

A laboratory apparatus was constructed to determine the transient thermal diffusivity of early-age Portland cement mortar using the proposed method. The experimental setup, shown in Fig. 1c, is a closed-loop system that requires two water baths that are controlled at different temperatures. A water reservoir is glued to the cell (the rectangular area containing the mortar, cell dimensions are $10\times10\times12$ cm) using a contact adhesive to make the cell watertight. Holes in the cell used to place thermocouples were also sealed. The inlet tube is connected to the pump that draws from a valve that selects either the hot or cold-water bath, while the outlet leads to a valve that sends the water back to its original reservoir. The valves are computer-controlled and switch every 10 min. This forces the left side of the cell to adopt a periodic temperature oscillation between the temperatures of the water baths. A thermocouple was dedicated to each water bath to make sure the water baths maintained their set temperatures of 35 °C and 50 °C throughout the course of the experiment.

Type T thermocouples were calibrated and then placed near the center of the cell at distances 1, 2, and 3 cm from the left

Table 1
Composition of Portland cement mortar used in the experiment

Ingredient	Mass per batch (g)
ASTM C150 type I cement	1496
ASTM C33 sand*	3399
Total free water	671

*Moisture content of sand=3.9%, absorption of sand=2.1%.

wall. After calibration, the thermocouples were verified to be accurate to ±0.1 °C. The true value of temperature is of secondary importance for the thermocouples. The ability of the thermocouples to measure changes in temperature, and hence the amplitude of the thermal oscillation, is of paramount importance to the overall accuracy of the results. The thermocouples maintained an accuracy of ±0.1 °C from 20 °C to 90 °C, verified in 10 °C increments. Therefore, the system can measure changes in temperature very accurately. The results shown in Section 4 are based on the 1-cm and 3-cm data. Temperature data was acquired every 10 s using an Agilent 34970A Data Acquisition/Switch Unit controlled by a computer running Microsoft Visual Basic Version 4.0. Thermal diffusivity can then be calculated from the attenuation of the amplitude of the temperature oscillation as a function of distance from the wall as described in Section 2.4.

The proposed method only works for solid or semi-solid materials because the calculations assume conductive heat transfer, and any convective heat transfer would result in significant errors. One example of a semi-solid which does not exhibit free convection would be a Portland cement mortar, which is often classified as a Bingham-plastic material, because it requires a yield stress to initiate flow. Since the driving forces for convection from these mild temperature gradients are very small, the authors assert that these forces should not be sufficient to overcome the yield stress and initiate a convective flow under ordinary circumstances. While continuous solids make ideal samples in theory, placing temperature sensors and achieving good thermal contact within solids is experimentally difficult. Solid particles, such as sand, readily fill the volume around the thermocouples for good thermal contact while exhibiting negligible convective heat transfer. For this reason, sand with various moisture contents was chosen as a standard to quantitatively test the system.

Therefore, the first material studied was ASTM C33 concrete sand. As received, the sand had a moisture content of 3.9 wt.% with an absorption of 2.1 wt.% and was considered "moist." Dry sand was defined as sand that was dried in an oven for 24 h. Wet sand was defined as sand that had been immersed in water and then drained briefly before the test.

After completion of the sand series of experiments, a mortar composition was chosen that is shown in Table 1. The mortar was mixed according to ASTM standard C 305 and placed and consolidated in the cell in thirds to minimize air voids. Two identical mortars were mixed in different batches, and their temperatures were monitored for one full week each. The thermal diffusivity was then extracted from the thermal history at the 1-cm and 3-cm positions using the data analysis techniques described in Section 2.4.

4. Results

4.1. Sand

The first material tested was the concrete sand. Table 2 shows results obtained for the wet, moist, and dry sand specimens compared to literature values. While sand is a suitable material for this analytical method, it is not an ideal standard material, since its material properties depend on the type, moisture content, particle size distribution, and packing among other factors. Nonetheless, Table 2 shows very good agreement between the experimental and published literature values [16]. The small discrepancies between the values may be accounted for by differences in the moisture conditions or any of the other aforementioned factors. The thermal diffusivity of dry sand calculated using the proposed method is plotted in Fig. 6 as a function of time. Although there is some deviation, the average value for thermal diffusivity remains constant as expected.

4.2. Mortar specimens

The moving-average value of thermal diffusivity is shown in Fig. 7a and b as a function of time after water addition for the two mortar blocks over 1 week. The standard deviation of the data is also shown. These values for thermal diffusivity are within the same range as typical literature values, which are often around 4×10^{-7} m^2/s [17], but can vary by an order of magnitude depending on the exact components, water content, proportions, mix procedure, age, and exposure conditions among other factors [5,6,13,18,19].

The thermal diffusivity exhibits a slight increase over the first day. Thermal diffusivity was found to increase 11–12% from 2 to 24 h after the time of water addition. Fig. 8 shows that a fourth-order polynomial can be fitted to the data for the first 24 h to extrapolate the thermal diffusivity of the initial time of water addition ($t=0$). The extrapolated value (5.7×10^{-7} m^2/s) can be obtained using a power law fit or any other polynomial fit of an order greater than two. These extrapolated values suggest that the thermal diffusivity may increase by 14–17% over the first 24 h from the initial mix. However, the total increase in thermal diffusivity may be as low as the 11–12% measured, since the first 2 h after mix correspond to a dormant period in the hydration reactions which may invalidate the extrapolation. The measured changes in thermal diffusivity generally coincide with the duration of the so-called slump-loss,

Table 2
Literature values compared to experimental values of thermal diffusivity for sand [16]

	Literature value ($m^2/s\times10^7$)	Experimental value ($m^2/s\times10^7$)	Standard deviation ($m^2/s\times10^7$)
Wet sand	7.43	7.49	0.19
Moist sand	8.40	8.39	0.41
Dry sand	2.33	1.70	0.04

Standard deviation of the experimental values is also listed.

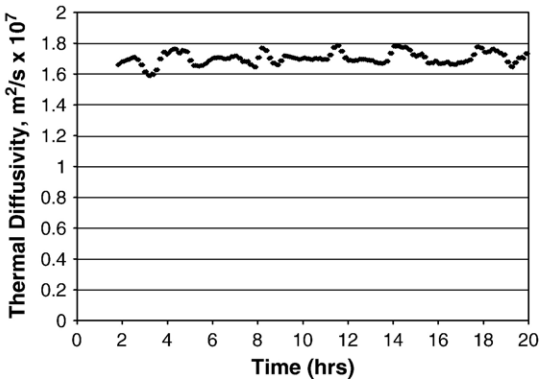

Fig. 6. Thermal diffusivity calculated for dry sand from experimental data.

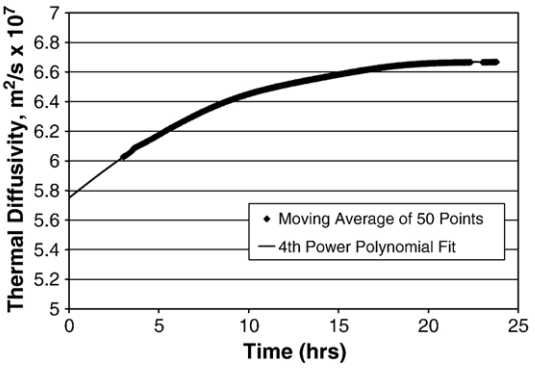

Fig. 8. Thermal diffusivity calculated for mortar during the first day. The fourth-order polynomial used to extrapolate the thermal diffusivity at the time of water addition ($t=0$) is also shown.

setting, and early hardening or "strength-gain" period over which cement based materials experience their most rapid changes in properties.

With the current precision of this method and apparatus, there is no statistically significant change detected in thermal diffusivity from the first day to the next 6 days. Changes might be detectable after the first 24 h if more precise instruments are assembled or if longer times are studied. Also, these cells are built to be closed systems, so the thermal diffusivity between 20 and 160 h may have remained approximately constant because the total moisture content was held constant. In actual construction applications, however, the thermal diffusivity over this time period may change considerably if the specimen is in open contact with the atmosphere due to water exchange with the environment. Table 2 shows that the thermal diffusivity of sand is extremely sensitive to moisture content, and the thermal diffusivity of mortar is also sensitive to moisture content and relative humidity [13].

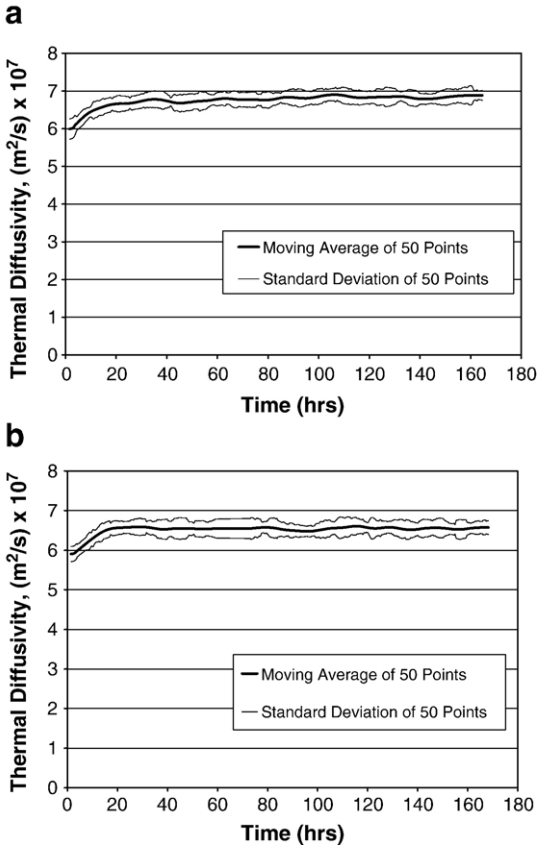

Fig. 7. a, b. Thermal diffusivity of two separate batches of mortar over the first week.

5. Discussion

The objective of this work is to investigate the effectiveness of this method for determining the thermal diffusivity of Portland cement mortars over a narrow temperature range and to ascertain advantages and limitations of this method. Computer simulation demonstrates that this method can yield accurate results despite the complications of internal heat generation and dependencies on temperature and time, even with non-sinusoidal inputs if Eq. (10) is used. As long as the frequency of the input temperature oscillation is significantly faster than changes in the rate of heat generation, the heat generation effects on the temperature profile ($T_g(x,t)$) can be subtracted as a baseline, leaving only the effects of the temperature oscillation induced by the external heat source ($T_{osc}(x,t)$).

Temperature dependence of thermal diffusivity could invalidate the method if it results in a significant change in the value over the amplitude range of the temperature oscillation (+/− 5 degrees C for this model and experiment). Implementing a large temperature dependence to the thermal conductivity in the computer simulation did not affect the accuracy of the diffusivity calculation. Eqs. (10) and (13) also implicitly assume that transient, start-up features of the waveform have become irrelevant. From Figs. 3b and 4b, this assumption is shown to be computationally effective after 1 h, yielding accurate values for thermal diffusivity.

Computer modeling of this problem has proven effective for testing assumptions in the experiment and data analysis. The validity of these assumptions depends on specific material tested and the apparatus used; however, testing these assumptions and optimizing the experimental design parameters with simple models is useful in any case.

Overall, this method has proven to be robust in its tolerance to the simplifying assumptions made. One notable advantage is

that the analysis yields two thermal diffusivity values for each oscillation, in this case, one output value per 10 min. This frequent data output allows for average values over time to be stated with greater certainty.

Also, this method keeps exothermic materials nearly isothermal near the temperature-controlled wall as seen in Figs. 3a and 4a. If analysis of a more strictly isothermal system is a priority for a particular application, then the calculations can be made from points nearer the wall. However, if the wall temperature input is not sinusoidal, then the error from the sinusoidal assumption upon which Eqs. (10) and (13) are based may increase as temperature measurements approach the wall, especially if the time-lag approach is used for the calculations.

Other major experimental design considerations include the frequency, input temperature amplitude, and the number and placement of thermocouples. Higher frequencies allow for the system to stabilize faster and yield more thermal diffusivity calculations over the duration of the experiment. Lower frequencies allow for greater temperature amplitudes within the sample, causing a higher signal-to-noise ratio for more accurate calculations. Higher temperature amplitudes also improve the signal-to-noise ratio, but makes the isothermal assumption poorer, which may be a problem if the material properties are temperature-dependent. This is particularly important in reacting systems, since most chemical reactions, which determine material properties, are highly temperature-dependent. Also, the accuracy has a second order dependence on the error in the distance between observation points. This requires the two thermocouples to be placed a sufficient distance apart so that this distance can be measured with a minimal relative error. However, both thermocouples must be placed close enough to the temperature-controlled wall so that they have an acceptable signal-to-noise ratio.

A similar apparatus might be configured to determine the thermal diffusivity of cement paste or concrete. Design considerations for cement paste would include sensor placement closer to the wall where the temperature stays closer to T_{avg}. A single measurement based on a 2-cm spacing between thermocouples used in many of these experiments may not be representative of the bulk properties of concrete due to the presence of coarse aggregate particles. Ideally, the sample should be homogenous on the size scale of the thermocouple spacing. Therefore, multiple thermocouple pairs with spacings larger than the coarse aggregate would be recommended for ascertaining the average thermal diffusivity of concrete.

Computer modeling can also be used to assess most of these design considerations effectively before building a laboratory apparatus if the thermal diffusivity is approximately known as the case was for this work. As a result, all of the tests yielded practical results on their initial runs because the design parameters were optimized using computer simulations beforehand. Therefore, anyone intending to use this method should consider Eq. (10) and similarly use computer modeling to validate assumptions and optimize experimental design parameters.

The focus of this work was to create, develop, and validate this method for measuring the thermal diffusivity of early-age mortars. If an appropriate apparatus is designed properly, this method could be applied to a wide range of other materials, including cement pastes, concrete, other chemically-reactive solids or semi-solids, or even biological tissues, where large temperature changes are also undesired and exothermic reactions complicate the analysis. The thermal properties of biological tissues have been previously determined by transient hot wire methods analogous to the methods used for mortar and concrete [20].

6. Conclusions

Monitoring the propagation of an oscillating temperature through a specimen has proven to be a robust method for determining the transient thermal diffusivity of Portland cement mortars. This method is tolerant to heat generation, imperfect sinusoidal temperature input, and temperature and time dependence of thermal diffusivity. This method is limited to solid, semi-solid, or extremely viscous materials because fluid flow results in convective heat transfer which invalidates the mathematical model. Applications could extend to a variety of other materials, including cement paste, concrete, or even biological tissue, where heat generation, transient physical properties, and narrow permissible temperature ranges complicate the study of their thermal properties. The optimal experimental design parameters, however, are highly dependent on the material studied and equipment available. Research in the near future will include running mortars at various compositions and types over a range of temperatures to collect a greater breadth of data on the transient thermal diffusivity of mortars.

Acknowledgements

This work was supported by the Intelligence Community Postdoctoral Research Fellowship Program. The authors would like to thank Dr. Cesar Chan for his help with the mortar mixing and characterization procedures. A great debt is owed to Tim Bond for his assistance in setting up the computer control and data acquisition systems. Saunders Concrete Company provided the Portland cement and concrete sand used in this study.

References

[1] G.J. Gibbon, Y. Ballim, Determination of the thermal conductivity of concrete during the early stages of hydration, Magazine of Concrete Research 50 (3) (1998) 229.
[2] P. Mounanga, A. Khelidj, G. Bastian, Experimental study and modelling approaches for the thermal conductivity evolution of hydrating cement paste, Advances in Cement Research 16 (3) (2004) 95–103.
[3] H.L. Lautz, Estimating Compressive Strength and Thickness of Concrete Based on Surface Temperature, in Civil and Environmental Engineering. Masters Thesis 2004, Cornell University: Ithaca, NY.
[4] A. Bouguerra, et al., The measurement of the thermal conductivity of solid aggregates using the transient plane source technique, Journal of Physics. D, Applied Physics 30 (20) (1997) 2900–2904.
[5] M.I. Khan, Factors affecting the thermal properties of concrete and applicability of its prediction models, Building and Environment 37 (6) (2002) 607.
[6] K.-H. Kim, et al., An experimental study on thermal conductivity of concrete, Cement and Concrete Research 33 (3) (2003) 363.

[7] S. Krishnaiah, D.N. Singh, Determination of thermal properties of some supplementary cementing materials used in cement and concrete, Construction and Building Materials 20 (3) (2006) 193–198.
[8] B.H. Low, S.A. Tan, T.F. Fwa, Determination of thermal-diffusivity of construction materials, Journal of Testing and Evaluation 19 (6) (1991) 440–449.
[9] A.K. Shrotriya, et al., Thermal-characteristics of some antigranulocytes construction materials at different temperatures, Indian Journal of Pure & Applied Physics 29 (5) (1991) 339–343.
[10] L.L. Sparks, Thermal conductivity of a concrete mortar from 95 K to 320 K, NASA STI/Recon Technical Report N, 82, vol. 24396, 1981, p. 17.
[11] M.G. VanGeem, J. Gajda, K. Dombrowski, Thermal properties of commercially available high-strength concretes, Cement Concrete and Aggregates 19 (1) (1997) 38–54.
[12] G. Deschutter, L. Taerwe, Specific-heat and thermal-diffusivity of hardening concrete, Magazine of Concrete Research 47 (172) (1995) 203–208.
[13] ACI Committee 122, Guide to Thermal Properties of Concrete and Masonry Systems, American Concrete Institute, Farmington Hills, MI, 2002.
[14] O.M. Alifanov, Inverse Heat Transfer Problems. International Series in Heat and Mass Transfer, Springer-Verlag, Berlin, 1994 xii, 348 pp.
[15] J.R. Welty, C.E. Wicks, R.E. Wilson, Fundamentals of Momentum, Heat, and Mass Transfer3rd ed., Wiley, New York, 1984 xxii, 803 pp.
[16] W.R.V. Wijk, Physics of plant environment. 1963, Amsterdam, New York: North-Holland Pub. Co.; Interscience Publishers. xvi, 382 p.
[17] Y.S. Xu, D.D.L. Chung, Effect of sand addition on the specific heat and thermal conductivity of cement, Cement and Concrete Research 30 (1) (2000) 59–61.
[18] W.N. dos Santos, Effect of moisture and porosity on the thermal properties of a conventional refractory concrete, Journal of the European Ceramic Society 23 (5) (2003) 745–755.
[19] B.M. Suleiman, Moisture effect on thermal conductivity of some major elements of a typical Libyan house envelope, Journal of Physics D (Applied Physics) 39 (3) (2006) 547.
[20] A. Bhattacharya, R.L. Mahajan, Temperature dependence of thermal conductivity of biological tissues, Physiological Measurement 24 (3) (2003) 769–783.